Received: 12 July 2023 | Revised: 17 August 2023 | Accepted: 17 August 2023

DOI: 10.1002/sia.7254

RESEARCH ARTICLE

SURFACE and INTERFACE ANALYSIS WILEY

# Photoelectron spectroscopy of ceria: Reduction, quantification and the myth of the vacancy peak in XPS analysis

David J. Morgan [1,2]

[1]Max Planck-Cardiff Centre on the Fundamentals of Heterogeneous Catalysis, Cardiff Catalysis Institute, Translational Research Hub, Cardiff University, Cardiff, UK

[2]HarwellXPS: The EPSRC National Facility for X-ray Photoelectron Spectroscopy, Research Complex at Harwell (RCaH), Didcot, UK

**Correspondence**
David J. Morgan.
Email: morgandj3@cardiff.ac.uk

**Funding information**
EPSRC National Facility for XPS ('HarwellXPS'), Grant/Award Number: PR16195

Primarily due to its inherent redox chemistry, ceria ($CeO_2$) is of use in many diverse areas of research. However, there is a wealth of misinterpretation of the oxygen spectra when discussing the result of damage or reduction to the $CeO_2$ lattice, especially with regard to a signal in this region attributed to oxygen vacancies. In this paper, it is shown that this peak cannot be due to vacancies and that a better understanding of the changes in stoichiometry of $CeO_2$ is best viewed from that of the Ce(III) component when considered in tandem with the O 1s signal.

**KEYWORDS**
$CeO_2$, ceria, oxygen, vacancy, XPS

## 1 | INTRODUCTION

There has been a recent drive to address the so-called reproducibility crisis in x-ray photoelectron spectroscopy (XPS)[1–3] with focused topics such as the use of correct standards and terminology,[4,5] peak fitting and data analysis[6–9] and sample handling[10] to name but a few. While these papers are a must-read for any practitioner of XPS, for novice users, there can still be a barrier to question quantified data which can lead to the propagation of errors in the literature. An example of this is a fundamental misunderstanding in what XPS can tell us about the oxygen states within a metal oxide.

In the O 1s spectrum, there are usually at least two oxygen signals. The first and typically most intense is the signal for the lattice oxygen atoms, with a binding energy generally in the range of 529–530 eV; however, there are exceptions such as $SiO_2$ where the signal is approximately 533 eV. The second higher energy peak, in the range 531–532 eV, is assigned as hydroxide or in many studies as 'oxygen vacancies'.

The published literature is littered with examples of researchers discussing oxygen vacancies in various materials through the presence of a supposed defect peak in the O 1s core-level spectra, which can be traced back to a paper by Fan and Goodenough discussing $In_2O_3$.[11] However, the entire basis of XPS as a technique is the measurement of the kinetic energy of a photoelectron ejected from an orbital, the proposition therefore that a specific peak is representative of a vacancy is preposterous, the very fact of there being a vacancy within the lattice means that there is simply no electron to be ejected and hence measured.

There have already been papers published addressing this erroneous assignment. For example, Idriss[12] has elegantly shown that through a review of the literature, the assignment of a peak as an oxygen vacancy is wrong, while recent computational studies by Frankcombe and Liu[13] again beautifully illustrate the fallacy of vacancy assignment in the case of ZnO.

In this paper, we focus on ceria, $CeO_2$, which mainly due to its redox properties finds use in a wide range of applications.[14–16] However, it is because of this redox chemistry that the presence of Ce(III) states is thought of as oxygen vacancies. In this paper, it is shown experimentally how to address the role of Ce(III) reduced states in ceria and related materials and quantify the stoichiometry of the defective ceria.

## 2 | EXPERIMENTAL

All data were collected using a Kratos Axis Ultra DLD photoelectron spectrometer using Al kα radiation (photon energy 1486.6 eV)

operating at 10 mA × 15 kV (150 W). To maximise sensitivity, while lowering acquisition time per cycle, the system was operated in the hybrid mode with the slot aperture, giving a total analysis area of approximately 700 × 300 µm.

The Ce 3d, O 1s and C 1s spectra were recorded at a pass energy of 40 eV and step size of 0.1 eV. The spectra were acquired sequentially over a total of 600 min, with each of the three regions taking approximately 2 min to acquire, giving approximately 6 min per iteration.

Charge compensation was performed using low-energy electrons flooding the ceria surface. The compensation system was operated with a filament current of 0.42 A, charge balance of 4.2 V and a filament bias of 1.4 V. Spectra are typically overcompensated by approximately 2–3 eV and hence corrected to the C 1s peak of adventitious carbon taken to be 284.8 eV. However, over the course of the experiment, the C 1s peak was found to vary by approximately 0.4 eV becoming an unreliable calibration point; therefore, the O 1s peak of the lattice oxygen was used and taken to be 529.7 eV. The C 1s spectra are shown in the supporting information Figure S1.

Data were calibrated and analysed using CasaXPS v2.3.26 rev1.1 K.[17] Quantification was performed using the Kratos F1s RSF library as supplied within the software. Background removal was achieved using a Shirley background, and peak fitting where required was performed using a Voigt-like function, defined within the software by LA(α,β,m) where broadly the first two parameters control the asymmetry of the high and low binding energy sides of the peak, while the third parameter specified the width of the Gaussian used to modify the Lorentzian curve, omission of the β parameter means it is equal to the α parameter. Generally, Ce(III) and O 1s components were fitted using LA(1.53,243), while the more asymmetric like components of the Ce(IV) spectra were fitted using LA(0.9,2,50). Peak shapes for $CeO_2$ were derived using a stoichiometric single crystal in which peak areas were constrained using the expected peak ratios, although the full width at half maximum (FWHM) were allowed to vary.

The $CeO_2$ powder (Alfa Aesar, 99.9% purity) was used as received and mounted in standard laboratory conditions by compacting into a recess of an in-house modified standard Kratos Axis Ultra sample bar using a clean glass microscope slide. The $CeO_2$ single crystal was obtained from PI-KEM (Tamworth, UK) and cleaned within the spectrometer using argon sputtering using a Kratos Minibeam 1 operating at 4 keV over a 5 × 5 mm raster area with an argon pressure of $10^{-6}$ mbar. A stoichiometric crystal (as confirmed by XPS quantification) was regenerated through heating to approximately 750°C in $10^{-5}$ mbar of oxygen.

## 2.1 | The photoelectron spectra of cerium oxides

Well-resolved cerium oxide spectra were first published by Burroughs et al.,[18] who showed, as have many authors since, the origin of the complex satellite structure inherent within these f-electron systems derived from ligand-to-metal charge transfer.[18,19] To discuss the reduction of ceria, we can familiarise ourselves with the spectra of $CeO_2$ and $Ce_2O_3$. The spectra shown in Figure 1 were acquired from a ceria single crystal and are labelled according to the nomenclature introduced in Burroughs et al.[18] Note that due to the absence of carbon on these surfaces, both spectra have been calibrated to the O 1s peak taken to be 529.7 eV.

For the $CeO_2$ spectrum, there is a total of six peaks, where the $u^{iii}$ and $v^{iii}$ peaks (917.0 and 898.3 eV, respectively) come from a Ce $3d^9 4f^0$ O $2p^6$ final state, while peaks u, v, $u^{ii}$, and $v^{ii}$ (901.2, 882.5, 907.8 and 889.2 eV, respectively) are a consequence of Ce $3d^9 4f^2$ O $2p^4$ and Ce $3d^9 4f^1$ O $2p^5$ final states.

For the representative $Ce_2O_3$ spectrum, the Ce(III) oxidation state exhibits four intense peaks; those labelled $u^i$ and $v^i$ have binding energies of 903.9 and 885.6 eV and attributable to a Ce $3d^9 4f^1$ O $2p^6$ final state, whereas the peaks $u^0$ and $v^0$ at 899.2 and 880.7, respectively, are a consequence of a Ce $3d^9 4f^2$ O $2p^5$ final state.

It is emphasised at this juncture that the spectra of that we are considering to be $Ce_2O_3$ are not a bulk or stoichiometric material and

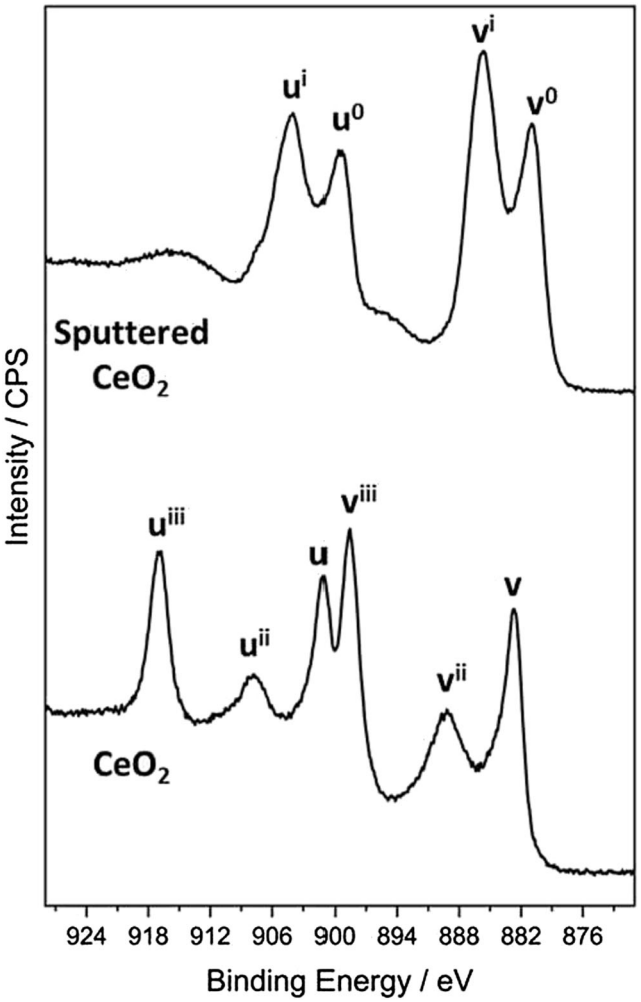


**FIGURE 1** The Ce 3d spectrum for $CeO_2$ and sputtered $CeO_2$ to mimic the $Ce_2O_3$ spectra. The peaks are labelled according to the nomenclature used by Burroughs et al.[18]

were created by sputtering the single crystal used for the $CeO_2$ spectrum. While this does yield Ce(III) spectra which are very similar to those previously attributed to $Ce_2O_3$ based mixed oxides,[20] $CePO_4$[21] and ion irradiated $CeO_2$,[22] care must be taken with regard to the intensity ratios between the $v^i + v^0$ peaks (and $u^i + u^0$ peaks) as variations have been noted in chelated Ce(III) species.[18]

Clearly, the presence of Ce(III) within a $CeO_2$ matrix will result in a very complex peak model, consisting of a total of 10 peaks where the concentration of Ce(IV) and Ce(III) can be found from the relative percentages of each set of peaks.[21–23]

## 2.2 | The myth of the oxygen vacancy peak in the XPS of ceria and related materials

For ceria, a distinct peak between 531 and 532 eV (depending on charge correction value) has been interpreted as oxygen vacancies,[24–30] the formation of $Ce_2O_3$,[31,32] or ambiguously defined as adsorbed oxygen species.[30,33–36] It is emphasised that these papers are not being singled out as the only ones that are erroneous in their assignment; indeed, as stated earlier, there are multiple examples in the literature. However, in these texts, little or no discussion is given to, for example, the C 1s spectrum which may indicate the presence of surface carbonate (although this may be somewhat complicated by the overlapping Ce 4s peak), or hydroxyl formation has not been considered. Certainly, metal hydroxides and carbonate typically have an O 1s signal in the binding energy range specified.[37,38] Furthermore, there is no reason to why $Ce_2O_3$ would have a higher O 1s binding energy than $CeO_2$, and both experimental[39,40] and computational[41] measurements have indicated little or no shift for the O 1s lattice signal.

## 2.3 | Assignment of chemistry through the controlled reduction of $CeO_2$

The reduction of $CeO_2$ during XPS analysis is not unknown,[19,20,42] and the formation of reduced states can be attributed to a number of physical and experimental phenomena.[43] However, the assignment of Ce(III) states is typically reported as defects or $Ce_2O_3$, without thought for actual assignment of the chemistry through a thorough analysis of the complimentary, but intrinsically linked Ce 3d and O 1s spectra.

Figure 2 shows Ce 3d and O 1s spectra taken at three different times from the prolonged exposure to X-ray analysis of a powdered $CeO_2$ sample. Without fitting, the increase in Ce(III) is clearly evident through the changes in the Ce 3d spectra, but note that there is little change in the O 1s spectrum. If, as claimed by some authors, the peak at 532 eV was due to $Ce_2O_3$, then the concentration of this would increase relative to the major O 1s lattice oxide component at 529.7 eV, so we can rule out this as an assignment.

Fitting of the Ce 3d spectra can be achieved using synthetic peak models, ideally taken from pure cerium compounds, through factor analysis[44] or an informed model approach.[45–47] This latter method provides an alternative to fitting spectra, by the inclusion of information from physical processes which affect the sample (such as X-ray degradation) without the need to identify synthetic line shapes. In these cases, spectral forms are extracted through continued analysis which are a representative shape constraint for reproduction of the spectral data. It is this latter method, which is used here, and the fitted spectra are shown in Figure 3. It should be noted that use of synthetic line shapes derived from the spectra in Figure 1 yields consistent results and is shown in Figure S2 of the supporting information.

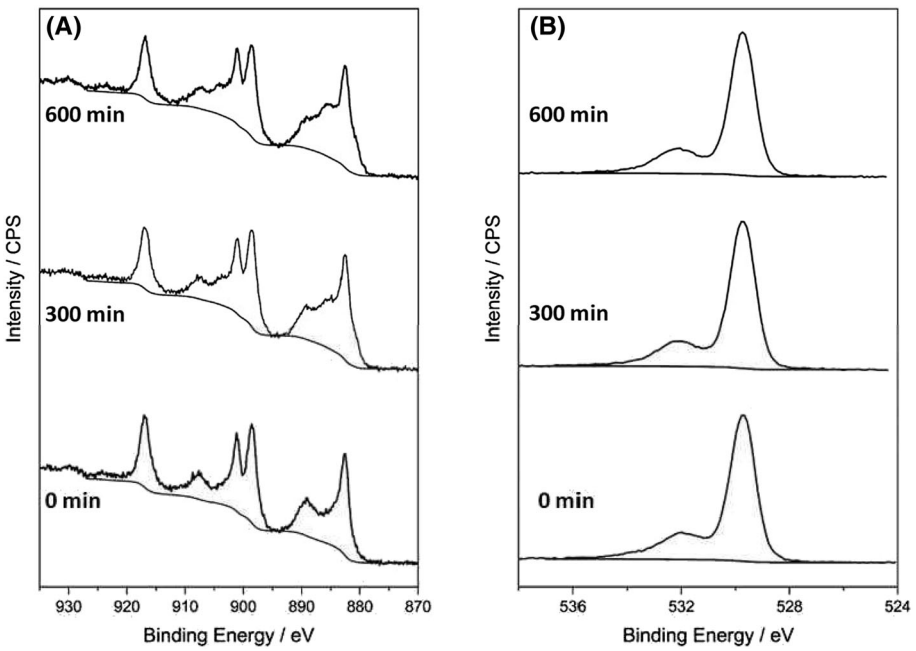


**FIGURE 2** (A) Ce 3d and (B) O 1s spectra taken from a series of spectral acquisitions totalling 600 min.

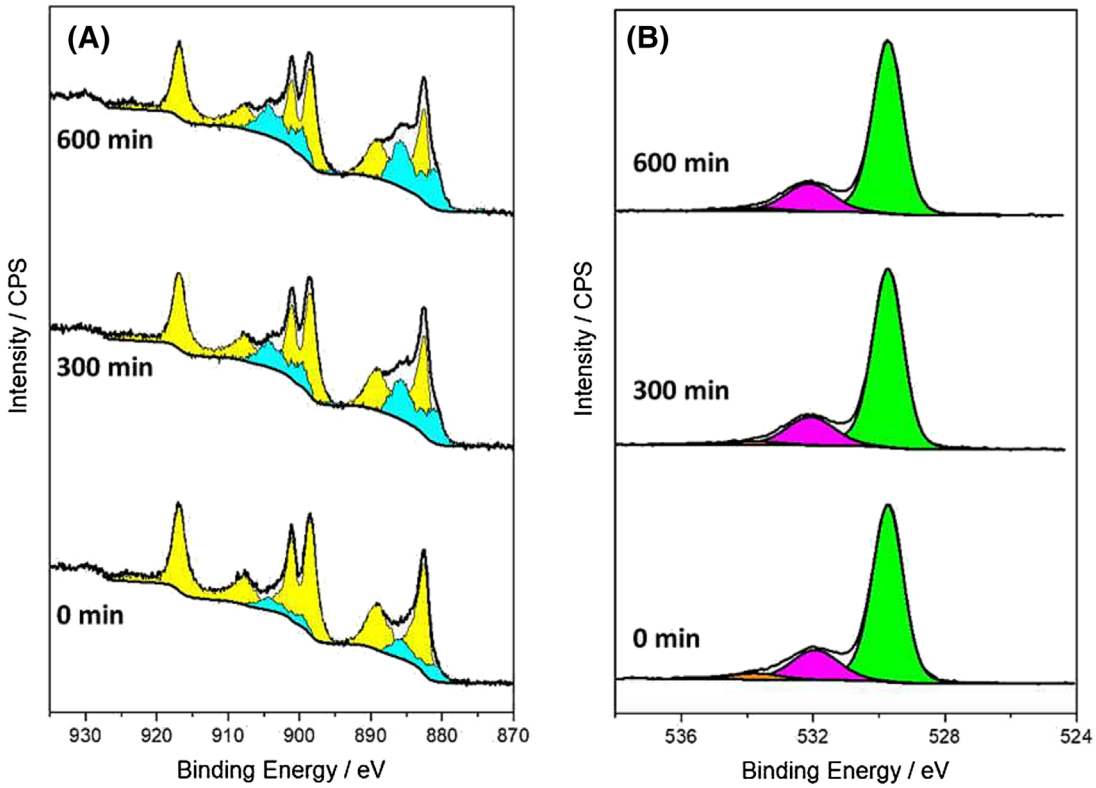


**FIGURE 3** (A) Ce 3d spectra fitted using the shapes derived from the informed sample model approach, where blue = Ce(III) and yellow = Ce (IV), and (B) O 1s spectra fitted with lattice oxide (green), hydroxide (magenta) and organic (orange) components.

**TABLE 1** The derived at% concentrations for Ce 3d and O 1s species at the three selected time frames.

| Time/min | Ce (IV) | Ce (III) | O 1s (529.7 eV) | O 1s (532.0 eV) | O 1s (533.7 eV) | Calculated stoichiometry |
|---|---|---|---|---|---|---|
| 0 | 27.88 | 4.50 | 52.12 | 12.70 | 2.79 | $CeO_{1.9}$ |
| 300 | 25.23 | 9.37 | 51.84 | 12.06 | 1.50 | $CeO_{1.7}$ |
| 600 | 24.19 | 11.17 | 51.05 | 12.15 | 1.44 | $CeO_{1.6}$ |

*Note*: Note that carbon has been omitted for clarity.

With fitting, the increase in Ce(III) is even more evident, but the question remains, how we can assign the peak at 532 eV so it is representative of the chemistry of the evolving ceria system? Considering the increase in the concentration of Ce(III) and the stability of the aforementioned O 1s peaks, the Ce(III) content cannot be solely a consequence of $Ce_2O_3$; instead, by using the complimentary data in the Ce 3d and O 1s spectra, it can be shown that the Ce(III) spectrum is a consequence of both $Ce_2O_3$ and $Ce(OH)_3$.

Table 1 shows the derived atomic concentrations for the cerium and oxygen chemical states, together with the calculated stoichiometry for the three times. By means of example, the derivation for $T = 300$ min is presented, while full derivations for the three times are given in the supporting information. Of course, the reasoning and analysis can be applied to the full reduction data set.

The peak above 533 eV is assigned to a small amount of surface contamination, which we note decreased between the first and remaining spectra which may suggest desorption of some surface species. Given its small concentration, and unlikely due to a Ce(III) or Ce(IV) species, this signal is ignored in the calculations discussed below.

Earlier, we discussed the binding energy of hydroxides and noted that they fall directly in the region 531–532 eV, so it is logical to first assume that this signal is due to surface hydroxide. Given the stoichiometry of the 1:3 ratio of Ce to OH and assuming that the signal at 532 eV is all hydroxide, then we can derive the Ce(III) contribution through the relationship:

$$\left[\mathrm{Ce(III)}_{\mathrm{hydroxide}}\right] = \frac{[\mathrm{O}_{532\,\mathrm{eV}}]}{3}$$

Therefore in our example, the concentration of Ce(III) due to the hydroxide is 4.02%. Our 'corrected' Ce(III) concentration is therefore

(9.37–4.02) = 5.35%. If we assume that this 5.35% is due to $Ce_2O_3$, then given the 2:3 stoichiometry, the percentage of oxygen in $Ce_2O_3$ is 1.5 time this concentration, in this case 8.03%.

Given the total lattice oxide concentration (51.84%), then the percentage due to Ce(IV) is (51.84–8.03) = 43.81%, and hence, the O/Ce (IV) ratio is 43.81/25.23 = 1.7 consistent with defective $CeO_2$, which could be described as $CeO_{1.7}$.

Repeating this calculation for the first and last sets of spectra, we find stoichiometries of $CeO_{1.9}$ and $CeO_{1.6}$, respectively, which support the reduction of $CeO_2$ through the increase in $Ce_2O_3$, but as shown by the full derivations given in the supporting information, it shows the majority of the Ce(III) states in the as-received oxide that are due to hydroxide groups.

In this model, we have of course assumed that the Ce(III) signal is composed of both stoichiometric hydroxide and oxide. Nevertheless, using the informed sample approach, we capture the total Ce(III) signal without the need for fitting synthetic peaks, and hence, we do not have to worry about any subtle differences which may exist in the ratios of the $v^0$ ($u^0$) and $v^i$ ($u^i$) peaks which may be present in the Ce 3d spectrum of $Ce_2O_3$ and $Ce(OH)_3$. It is noted that the change in the stoichiometry of the $CeO_2$ is small; however, it does show that prolonged analysis can lead to changes in the spectra and expected ratios and that this method of analysis reveals an explainable trend in the increase of Ce(III) within the Ce(IV) oxide lattice with the surface terminated by Ce(III) hydroxide and hence a more consistent measure of chemistry at the surface and the degree of nonstoichiometry in the near surface region of $CeO_2$.

## 3 | CONCLUSIONS

This work has sought to highlight the now increasingly documented erroneous assignment of peaks as oxygen vacancies. It has been shown that through careful consideration of the Ce 3d and O 1s levels together, coupled with an appreciation of the different oxygen states possible, the decrease in the O:Ce ratio in ceria can be followed and the Ce(III) chemistry can be assigned to both the oxide and hydroxide. It is hoped that this work, together with the papers of Idriss[12] and Frankcombe,[13] will facilitate an improved interpretation of O 1s spectra for oxide materials.

### ACKNOWLEDGEMENTS

XPS data collection was performed at the EPSRC National Facility for XPS ('HarwellXPS'), operated by Cardiff University and UCL, under contract no. PR16195.

### DATA AVAILABILITY STATEMENT

The data that support the findings of this study are openly available in the Zenodo repository (https://doi.org/10.5281/zenodo.8119279).

### ORCID

*David J. Morgan* https://orcid.org/0000-0002-6571-5731

### REFERENCES

1. Baer DR, McGuire GE, Artyushkova K, Easton CD, Engelhard MH, Shard AG. Introduction to topical collection: reproducibility challenges and solutions with a focus on guides to XPS analysis. *J Vac Sci Technol A*. 2021;39(2):021601. doi:10.1116/6.0000873
2. Baer DR, Watts JF, Herrera-Gomez A, Gaskell KJ. Evolving efforts to maintain and improve XPS analysis quality in an era of increasingly diverse uses and users. *Surf Interface Anal*. 2023;55(6–7):480-488. doi:10.1002/sia.7194
3. Major GH, Avval TG, Moeini B, et al. Assessment of the frequency and nature of erroneous x-ray photoelectron spectroscopy analyses in the scientific literature. *J Vac Sci Technol a*. 2020;38(6):061204. doi:10.1116/6.0000685
4. Baer DR, Shard AG. Role of consistent terminology in XPS reproducibility. *J Vac Sci Technol A*. 2020;38(3):031203. doi:10.1116/6.0000016
5. Unger WES. International standardization and metrology as tools to address the comparability and reproducibility challenges in XPS measurements. *J Vac Sci Technol A*. 2020;38(2):021201. doi:10.1116/1.5131074
6. Easton CD, Kinnear C, McArthur SL, Gengenbach TR. Practical guides for x-ray photoelectron spectroscopy: analysis of polymers. *J Vac Sci Technol a*. 2020;38(2):023207. doi:10.1116/1.5140587
7. Shard AG. Practical guides for x-ray photoelectron spectroscopy: quantitative XPS. *J Vac Sci Technol A*. 2020;38(4):041201. doi:10.1116/1.5141395
8. Tougaard S. Practical guide to the use of backgrounds in quantitative XPS. *J Vac Sci Technol a*. 2021;39(1):011201. doi:10.1116/6.0000661
9. Major GH, Fairley N, Sherwood PMA, et al. Practical guide for curve fitting in x-ray photoelectron spectroscopy. *J Vac Sci Technol a*. 2020;38(6):061203. doi:10.1116/6.0000377
10. Stevie FA, Garcia R, Shallenberger J, Newman JG, Donley CL. Sample handling, preparation and mounting for XPS and other surface analytical techniques. *J Vac Sci Technol A*. 2020;38(6):063202. doi:10.1116/6.0000421
11. Fan JCC, Goodenough JB. X-ray photoemission spectroscopy studies of Sn-doped indium-oxide films. *J Appl Phys*. 1977;48(8):3524-3531. doi:10.1063/1.324149
12. Idriss H. On the wrong assignment of the XPS O1s signal at 531–532 eV attributed to oxygen vacancies in photo- and electro-catalysts for water splitting and other materials applications. *Surf Sci*. 2021;712:121894. doi:10.1016/j.susc.2021.121894
13. Frankcombe TJ, Liu Y. Interpretation of oxygen 1s X-ray photoelectron spectroscopy of ZnO. *Chem Mater*. 2023;35(14):5468-5474. doi:10.1021/acs.chemmater.3c00801
14. Trovarelli A. *Catalysis by Ceria and Related Materials*. Published by Imperial College Press and Distributed by World Scientific Publishing Co.; 2002. doi:10.1142/p249
15. Trovarelli A. Catalytic properties of ceria and $CeO_2$-containing materials. *Catal Rev*. 1996;38(4):439-520. doi:10.1080/01614949608006464
16. Abiade JT, Yeruva S, Choi W, Moudgil BM, Kumar D, Singh RK. A tribochemical study of ceria-silica interactions for CMP. *J Electrochem Soc*. 2006;153(11):G1001. doi:10.1149/1.2349357
17. Fairley N, Fernandez V, Richard-Plouet M, et al. Systematic and collaborative approach to problem solving using X-ray photoelectron spectroscopy. *Appl Surf Sci Adv*. 2021;5:100112. doi:10.1016/j.apsadv.2021.100112
18. Burroughs P, Hamnett A, Orchard AF, Thornton G. Satellite structure in the X-ray photoelectron spectra of some binary and mixed oxides of lanthanum and cerium. *J Chem Soc Dalton Trans*. 1976;17(17):1686. doi:10.1039/dt9760001686
19. Paparazzo E, Ingo GM, Zacchetti N. X-ray induced reduction effects at $CeO_2$ surfaces: an x-ray photoelectron spectroscopy study. *J Vac Sci Technol A*. 1991;9(3):1416-1420. doi:10.1116/1.577638

20. Paparazzo E. XPS studies of damage induced by X-ray irradiation on $CeO_2$ surfaces. *Surf Sci*. 1990;234(1–2):L253-L258. doi:10.1016/0039-6028(90)90658-U
21. Bêche E, Charvin P, Perarnau D, Abanades S, Flamant G. Ce 3d XPS investigation of cerium oxides and mixed cerium oxide ($Ce_xTi_yO_z$). *Surf Interface Anal*. 2008;40(3–4):264-267. doi:10.1002/sia.2686
22. Maslakov KI, Teterin YA, Popel AJ, et al. XPS study of ion irradiated and unirradiated $CeO_2$ bulk and thin film samples. *Appl Surf Sci*. 2018;448:154-162. doi:10.1016/j.apsusc.2018.04.077
23. Paparazzo E. On the curve-fitting of XPS Ce(3d) spectra of cerium oxides. *Mater Res Bull*. 2011;46(2):323-326. doi:10.1016/j.materresbull.2010.11.009
24. López JM, Gilbank AL, García T, Solsona B, Agouram S, Torrente-Murciano L. The prevalence of surface oxygen vacancies over the mobility of bulk oxygen in nanostructured ceria for the total toluene oxidation. *Appl Catal B*. 2015;174–175:403-412. doi:10.1016/j.apcatb.2015.03.017
25. Sapkota P, Aprahamian A, Chan KY, et al. Irradiation-induced reactions at the $CeO_2/SiO_2/Si$ interface. *J Chem Phys*. 2020;152(10):104704. doi:10.1063/1.5142619
26. Ma R, Jahurul Islam M, Amaranatha Reddy D, Kim TK. Transformation of $CeO_2$ into a mixed phase $CeO_2/Ce_2O_3$ nanohybrid by liquid phase pulsed laser ablation for enhanced photocatalytic activity through Z-scheme pattern. *Ceram Int*. 2016;42(16):18495-18502. doi:10.1016/j.ceramint.2016.08.186
27. Wang M, Shen M, Jin X, et al. Oxygen vacancy generation and stabilization in $CeO_{2-x}$ by Cu Introduction with improved $CO_2$ photocatalytic reduction activity. *ACS Catal*. 2019;9(5):4573-4581. doi:10.1021/acscatal.8b03975
28. Ni Z, Djitcheu X, Gao X, Wang J, Liu H, Zhang Q. Effect of preparation methods of $CeO_2$ on the properties and performance of $Ni/CeO_2$ in $CO_2$ reforming of $CH_4$. *Sci Rep*. 2022;12(1):5344. doi:10.1038/s41598-022-09291-w
29. Xu W, Xu Z, Yao W, et al. Directly synthesis of dimethyl carbonate from $CO_2$ and methanol over UiO-66@$CeO_2$ catalyst. *Appl Catal Gen*. 2023;662:119262. doi:10.1016/j.apcata.2023.119262
30. Tang X, Zhang B, Li Y, Xu Y, Xin Q, Shen W. CuO/CeO2 catalysts: redox features and catalytic behaviors. *Appl Catal Gen*. 2005;288(1–2):116-125. doi:10.1016/j.apcata.2005.04.024
31. Wang L, Yu Y, He H, Zhang Y, Qin X, Wang B. Oxygen vacancy clusters essential for the catalytic activity of $CeO_2$ nanocubes for o-xylene oxidation. *Sci Rep*. 2017;7(1):12845. doi:10.1038/s41598-017-13178-6
32. Zhang J, Wong H, Yu D, Kakushima K, Iwai H. X-ray photoelectron spectroscopy study of high-k $CeO_2/La_2O_3$ stacked dielectrics. *AIP Adv*. 2014;4(11):117117. doi:10.1063/1.4902017
33. Yang M, Shen G, Wang Q, et al. Roles of oxygen vacancies of $CeO_2$ and Mn-doped $CeO_2$ with the same morphology in benzene catalytic oxidation. *Molecules*. 2021;26(21):6363. doi:10.3390/molecules26216363
34. Liu Y, Zhou Y, Ke Q, et al. Enhanced catalytic oxidation of diluted ethylene oxide on $Pt/CeO_2$ catalyst under low temperature. *Appl Catal Gen*. 2022;639:118642. doi:10.1016/j.apcata.2022.118642
35. Wei X, Li K, Zhang X, et al. $CeO_2$ nanosheets with anion-induced oxygen vacancies for promoting photocatalytic toluene mineralization: toluene adsorption and reactive oxygen species. *Appl Catal B*. 2022;317:121694. doi:10.1016/j.apcatb.2022.121694
36. Xiao M, Han D, Yang X, et al. Ni-doping-induced oxygen vacancy in Pt-$CeO_2$ catalyst for toluene oxidation: enhanced catalytic activity, water-resistance, and $SO_2$-tolerance. *Appl Catal B*. 2023;323:122173. doi:10.1016/j.apcatb.2022.122173
37. Shchukarev A, Korolkov D. XPS study of group IA carbonates. *Open Chem*. 2004;2(2):347-362. doi:10.2478/BF02475578
38. Stoch J, Gablankowska-Kukucz J. The effect of carbonate contaminations on the XPS O 1s band structure in metal oxides. *Surf Interface Anal*. 1991;17(3):165-167. doi:10.1002/sia.740170308
39. Praline G, Koel BE, Hance RL, Lee H-I, White JM. X-ray photoelectron study of the reaction of oxygen with cerium. *J Electron Spectros Relat Phenomena*. 1980;21(1):17-30. doi:10.1016/0368-2048(80)85034-1
40. Barr TL, Fries CG, Cariati F, Bart JCJ, Giordano N. A spectroscopic investigation of cerium molybdenum oxides. *J Chem Soc Dalton Trans*. 1983;9(9):1825. doi:10.1039/dt9830001825
41. Bosio N, Schaefer A, Grönbeck H. Can oxygen vacancies in ceria surfaces be measured by O1s photoemission spectroscopy? *J Phys Condens Matter*. 2022;34(17):174004. doi:10.1088/1361-648X/ac4f7b
42. Rama Rao MV, Shripathi T. Photoelectron spectroscopic study of X-ray induced reduction of $CeO_2$. *J Electron Spectros Relat Phenomena*. 1997;87(2):121-126. doi:10.1016/S0368-2048(97)00087-X
43. Morgan DJ. XPS insights: sample degradation in X-ray photoelectron spectroscopy. *Surf Interface Anal*. 2023;55(5):331-335. doi:10.1002/sia.7205
44. Holgado JP, Alvarez R, Munuera G. Study of $CeO_2$ XPS spectra by factor analysis: reduction of CeO2. *Appl Surf Sci*. 2000;161(3–4):301-315. doi:10.1016/S0169-4332(99)00577-2
45. Garland BM, Fairley N, Strandwitz NC, Thorpe R, Bargiela P, Baltrusaitis J. A study of in situ reduction of $MoO_3$ to $MoO_2$ by X-ray photoelectron spectroscopy. *Appl Surf Sci*. 2022;598:153827. doi:10.1016/j.apsusc.2022.153827
46. Baltrusaitis J, Mendoza-Sanchez B, Fernandez V, et al. Generalized molybdenum oxide surface chemical state XPS determination via informed amorphous sample model. *Appl Surf Sci*. 2015;326:151-161. doi:10.1016/j.apsusc.2014.11.077
47. Fernandez V, Kiani D, Fairley N, Felpin F-X, Baltrusaitis J. Curve fitting complex X-ray photoelectron spectra of graphite-supported copper nanoparticles using informed line shapes. *Appl Surf Sci*. 2020;505:143841. doi:10.1016/j.apsusc.2019.143841


## SUPPORTING INFORMATION

Additional supporting information can be found online in the Supporting Information section at the end of this article.

**How to cite this article:** Morgan DJ. Photoelectron spectroscopy of ceria: Reduction, quantification and the myth of the vacancy peak in XPS analysis. *Surf Interface Anal*. 2023; 1-6. doi:10.1002/sia.7254